

# THE X-RAY COUNTERPART OF THE HIGH-*B* PULSAR PSR J0726–2612

J. S. SPEAGLE<sup>1,2</sup>, D. L. KAPLAN<sup>1,3</sup>, AND M. H. VAN KERKWIJK<sup>4</sup>

*ApJ*, in press

## ABSTRACT

Middle-aged, cooling neutron stars are observed both as relatively rapidly spinning radio pulsars and as more slowly spinning, strongly magnetized isolated neutron stars (INSs), which stand out by their thermal X-ray spectra. The difference between the two classes may be that the INSs initially had much stronger magnetic fields, which decayed. To test this, we used the *Chandra X-ray Observatory* to observe 1RXS J072559.8–261229, a possible X-ray counterpart to PSR J0726–2612, which, with its 3.44 s period and  $3 \times 10^{13}$  G inferred magnetic field strength, is the nearest and least extincted among the possible slowly-spinning, strong-field INS progenitors (it likely is in the Gould Belt, at  $\sim 1$  kpc). We confirm the identification and find that the pulsar has a spectrum consistent with being purely thermal, with blackbody temperature  $kT = 87 \pm 5$  eV and radius  $R = 5.7^{+2.6}_{-1.3}$  km at a distance of 1 kpc. We detect sinusoidal pulsations at twice the radio period with a semi-amplitude of  $27 \pm 5\%$ . The properties of PSR J0726–2612 strongly resemble those of the INSs, except for its much shorter characteristic age of 200 kyr (instead of several Myr). We conclude that PSR J0726–2612 is indeed an example of a young INS, one that started with a magnetic field strength on the low end of those inferred for the INSs, and that, therefore, decayed by a relatively small amount. Our results suggest that the long-period, strong-field pulsars and the INSs are members of the same class, and open up new opportunities to understand the puzzling X-ray and optical emission of the INSs through radio observations of PSR J0726–2612.

*Subject headings:* stars: individual (PSR J0726–2612) — stars: neutron — X-rays: stars — X-rays: individual (1RXS J072559.8–261229)

## 1. INTRODUCTION

The *ROSAT* All-Sky Survey (RASS; Voges et al. 1999) showed that our census of cooling, nearby neutron stars was incomplete: it contained not just the known cooling pulsars such as PSR B0656+14 and Geminga, but also seven “isolated neutron stars” (INSs). These are nearby ( $\lesssim 1$  kpc), young ( $\lesssim 1$  Myr), cooling neutron stars with thermal X-ray spectra, long periods ( $> 3$  s), faint optical counterparts, and no detected radio emission (for reviews, see Haberl 2007; Kaplan 2008). The INSs are interesting both because of their abundance and because of the promise of inferring neutron-star parameters from their thermal emission. Unfortunately, despite large investments of time with *Chandra* and *XMM-Newton*, the nature of the emission remains puzzling, and we still understand neither the composition nor state (gaseous, condensed) of the surface.

A clearer picture has emerged for the origin and abundance of the INSs: most likely, they were born with very strong magnetic fields, of  $\gtrsim 10^{13.5}$  G, which decayed. Empirical evidence for this comes from our X-ray timing efforts (Kaplan & van Kerkwijk 2005a,b, 2009a,b, 2011; van Kerkwijk & Kaplan 2008), which showed that the current field strengths of the INSs are remarkably similar, in the range 1.0 to  $3.5 \times$

$10^{13}$  G, and that their characteristic ages of several Myr are substantially in excess of true ages of  $\sim 0.5$  Myr inferred from cooling and kinematics (Walter 2001; Motch et al. 2005; Kaplan, van Kerkwijk, & Anderson 2007; van Kerkwijk & Kaplan 2008; Motch et al. 2009; Tetzlaff et al. 2010, 2011). The long periods and characteristic ages follow naturally if the INSs initially had much stronger fields and thus faster spindown, and the similar current field strengths can be understood if fields stop decaying at a common value. Indeed, this was predicted theoretically by Pons, Miralles, & Geppert (2009): for initially weak magnetic fields, field decay leads to only a factor  $\sim 2$  change that is essentially unnoticeable (Popov et al. 2010), while for fields above  $10^{13}$  G field decay becomes increasingly important, with predicted final fields that are always a few  $\times 10^{13}$  G, independent of the initial values. The field-decay induced heating may also help explain the observed preponderance of INSs compared to “normal” middle-aged pulsars (Kaplan & van Kerkwijk 2009a; Faucher-Giguère & Kaspi 2006; Kaspi 2010).

If the above is correct, the progenitors of the INSs would have been neutron stars with fields ranging from  $\sim 5$  to  $50 \times 10^{13}$  G. The most magnetized would correspond to magnetars, but many would not be so energetic. Still, as their fields decay on  $\sim 100$  kyr timescales, they should be brighter than expected from simple cooling, and there should be a population of relatively long-period, strong-field sources that are anomalously hot. Verifying this might not only confirm the hypothesis for the INS population, but also yield clues to their emission: with the higher temperatures and stronger magnetic fields, one might expect the surface to have a dif-

<sup>1</sup> Physics Dept., U. of Wisconsin - Milwaukee, Milwaukee WI 53211, USA; kaplan@uwm.edu

<sup>2</sup> Current address: Harvard College, Cambridge, MA 02138, USA; joshuaspeagle@college.harvard.edu

<sup>3</sup> Corresponding author.

<sup>4</sup> Department of Astronomy and Astrophysics, University of Toronto, 60 St. George Street, Toronto, ON M5S 3H8, Canada; mhvk@astro.utoronto.ca

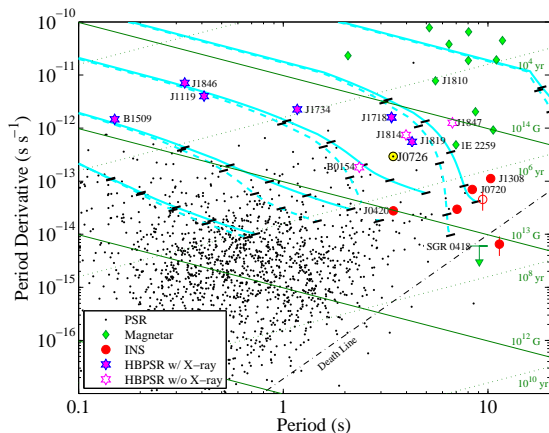


FIG. 1.—  $P-\dot{P}$  diagram, with known pulsars shown by dots, and strong-field populations highlighted (isolated neutron stars: red circles; magnetars: green diamonds; strong-field pulsars with X-ray observations: magenta stars [filled: detected; open: upper limit only]). Sources referred to in the text are labeled, as are lines of constant magnetic field, lines of constant characteristic age, and an approximate death line. Overlaid on the diagram are the predicted spin-down tracks from the field decay model of Pons et al. (2009) (solid lines: dipole only; dashed lines: including a toroidal component with a strength of 50 times that of the dipole). The initial dipole fields are  $10^{13,13.5,14,14.5,15}$  G at the pole, and there are cross-ticks at (0.01, 0.03, 0.1, 0.3, 1) Myr. We assumed initial periods of 0.1 s, and divided the field at the pole by two to get the field at the equator for comparison with the spin-down field estimates. For low field strengths, field decay is not important, and hence the tracks essentially follow constant-field lines (shown by the diagonal thin solid lines), and at any moment the characteristic age (diagonal thin dotted lines) is a reasonable estimate for the true age. For strong fields, however, field decay is important, and the field and characteristic age inferred at any moment are not representative for the initial field and true age.

ferent state and the spectra to show different spectral features that could be contrasted to the INNs.

Checking the  $P-\dot{P}$  diagram for possible INS progenitors (Fig. 1), one finds four radio pulsars, one rotating radio transient (RRAT), and one relatively low-field anomalous X-ray pulsar (AXP); all have periods longer than 3 s and fields in excess of  $3 \times 10^{13}$  G. Of course, the AXP (1E 2259+586), like other magnetars, is thought to be powered by magnetic field decay; it certainly is anomalously hot, with  $kT \simeq 0.4$  keV (Zhu et al. 2008). Of the others, the RRAT and one of the pulsars have X-ray counterparts as well, with thermal spectra and inferred temperatures of 140 – 190 eV (PSR J1718–3817, Kaspi & McLaughlin 2005; Zhu et al. 2011; PSR J1819–1458, McLaughlin et al. 2007). These temperatures are, as the authors mention, well above expectations from simple cooling (and also well above the limit of  $\sim 70$  eV inferred for PSR B0154+61 (Gonzalez et al. 2004), a young pulsar with a somewhat weaker inferred field; see Fig. 1). The best-studied source, PSR J1819–1458, also has a clear absorption feature at 1 keV, well above the energies at which absorption is seen in the INNs. Among the three remaining sources, PSR J1814–1744 and PSR J1847–0130 have unpublished, reasonably long *XMM* observations. We checked these and found no counterparts, but as both pulsars are distant and extincted, this is not unexpected. Indeed all of these objects are considerably further than the INNs, and while part of this can be explained by their small ages leading to lower space densities, part comes from

the narrowly-beamed/intermittent radio emission that is used to detect them (compared to omni-directional soft X-rays).

The last source, PSR J0726–2612 (hereafter PSR J0726) is the subject of this paper. This 3.44 s pulsar was discovered in the course of the Parkes High-Latitude survey (Burgay et al. 2006) but surprisingly has not seen any X-ray follow-up, despite its inferred magnetic field of  $B = 3 \times 10^{13}$  G and characteristic age of only  $\tau \equiv P/2\dot{P} = 200$  kyr. Yet, it is arguably the most interesting, since it should be the least extincted — both because it has the lowest dispersion measure (DM) of all (70 vs. 200 to 800  $\text{cm}^{-3} \text{pc}$  for the other four pulsars) and because it is at what is, for a young pulsar, high Galactic latitude ( $|b^{\text{II}}| = 4.7^\circ$  vs.  $< 0.22^\circ$  for the others). Furthermore, it may well be the closest. From its dispersion measure, combined with a model of the Galactic electron distribution (Cordes & Lazio 2002), one infers a rough distance of 3 kpc. But at that distance, its height above the Galactic plane is 250 pc, which is somewhat improbable. A more likely alternative is that it is at  $\sim 1$  kpc, situated (and born) in the Gould Belt (Popov et al. 2005), which this line of sight passes through (and which may influence the dispersion measure). Below, we will scale our distances to  $d_{\text{kpc}} = d/1 \text{ kpc}$ .

Overall, PSR J0726 seems a prime candidate for comparison with the INNs, being relatively close and unabsorbed, and apparently intermediate between the stronger-field pulsars that look most like INS progenitors and the weak-field normal pulsars that form the bulk of the population. Intriguingly, we found a possible counterpart to PSR J0726 in the RASS: 1RXS J072559.8–261229, with  $0.027 \pm 0.011 \text{ ct s}^{-1}$ . The nominal separation of  $112''$  from the pulsar is relatively large, but in the RASS image, the source seemed somewhat extended, encompassing the pulsar. Here, we present a *Chandra X-ray Observatory* of 1RXS J072559.8–261229 that confirms the identification with PSR J0726, and allows a first comparison between PSR J0726 and the INNs, opening the way for detailed followup.

## 2. OBSERVATIONS & ANALYSIS

We observed PSR J0726 with the Advanced CCD Imaging Spectrometer (ACIS; Garmire et al. 2003) aboard the *Chandra X-ray Observatory* (CXO; Weisskopf et al. 2000) on 2011 June 15 for 17.9 ks (ObsID 12558). For best sensitivity at low energies, we used the back-illuminated S3 CCD, selecting the 1/8-subarray read-out mode (with 0.4 s sampling) to resolve the 3-s pulse period. We processed the level-1 event lists following standard procedures (using `chandra_repro` from CIAO v4.3 and CALDB v4.4.5). The data show one clear source, with a J2000 position (from `celldetect`)  $\alpha = 07^{\text{h}}26^{\text{m}}08^{\text{s}}.14$ ,  $\delta = -26^\circ 12' 38''.7$  with an uncertainty dominated by the boresight error of  $\sim 0''.6$  (90% confidence). This is consistent with the radio position of PSR J0726 in the ATNF pulsar catalog (Manchester et al. 2005):  $\alpha = 07^{\text{h}}26^{\text{m}}08^{\text{s}}.12 \pm 0''.04$ ,  $\delta = -26^\circ 12' 38''.1 \pm 0''.8$ .

For our further analysis, we selected 1179 source events from a circular region with a radius of 5 pixels ( $2''.46$ ), encompassing  $> 95\%$  of the source photons, and 326 background events from the rest of the detector area (a factor of 1200 larger in area), with energies between 220 eV

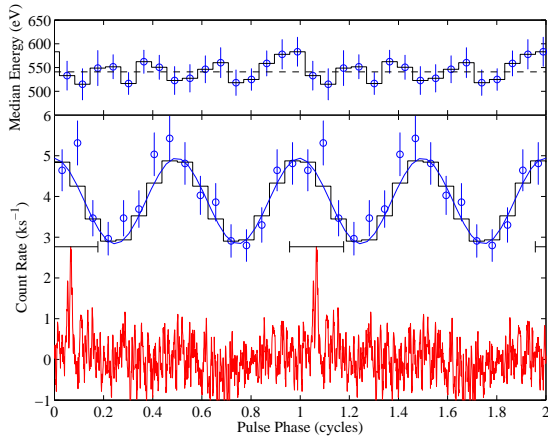


FIG. 2.— Lower panel: X-ray (blue) and radio (red) pulse profiles of PSR J0726–2612. The X-ray data are from our new *Chandra* observations, while the radio data are from the ATNF pulsar data archive with an arbitrary flux offset and scaling (these are from a 152-s observation centered at 1374 MHz with 288 MHz bandwidth, taken on 2005 March 26). Both pulses are repeated twice for clarity. The uncertainty on the X-ray TOA is 0.013 cycles, but in comparing that to the radio TOA we must include the uncertainties on the ephemeris which contribute substantially. The apparent shift between the radio and X-ray pulses is  $0.07 \pm 0.11$  cycles, as shown by the black error bars. Upper panel: the median energy in each phase bin.

(the recommended lower-bound for data from the ACIS; any lower and the calibration becomes unreliable and soft flares become increasingly dominant) and 1.1 keV (where the effects of higher-energy flares are minimized; the source is barely detected above 1.1 keV). We corrected the event times to the Solar System barycenter using `axbary`, assuming the radio position.

### 2.1. Timing Analysis

To look for X-ray pulsations, we first determined the frequency that maximized the power in a  $Z_1^2$  periodogram (Rayleigh statistic; Buccheri et al. 1983) at different multiples of the radio frequency. We found no obvious peak at the expected frequency of the pulsar ( $Z_1^2 = 0.7$ ), but a strong one ( $Z_1^2 = 21.7$ ) at roughly double the frequency,  $0.290493 \pm 0.000002$  Hz (where the uncertainty was calculated following Ransom 2001). We found no evidence for significant power in higher harmonics ( $Z_1^2 = 1.2$  and  $0.70$  at the third and fourth harmonic, respectively). We folded our data on half our best-fit frequency to construct a binned light-curve (with 16 phase bins; Figure 2). As expected from the lack of other harmonics, a sinusoid provided a good fit ( $\chi^2 = 11.7$  for 13 degrees of freedom [dof]), with a pulsed fraction (semi-amplitude) of  $27\% \pm 5\%$ . The implied TOA, defined as the maximum of the sinusoid closest to the middle of the observation, is  $\text{MJD } 55727.6883125 \pm 0.0000006$ . The ephemeris in the ATNF catalog (based on data from 2005–2006) predicts a frequency of  $0.29049679119 \pm 9.6 \times 10^{-10}$  Hz at the epoch of our observation, which differs by  $\sim 2\sigma$  from our measurement. Further radio observations would help determine whether this is due to chance or due to something intrinsic (a glitch or timing noise).

In order to compare the phase of the radio and X-ray pulses, we retrieved an archived Parkes observation of PSR J0726 from 2005 March 26. The pulse profile, shown in Fig. 2, was substantially noisier than that

shown in Burgay et al. (2006), but still sufficed to determine a TOA. From the highest point in the profile, we find  $\text{MJD } 53455.29291874 \pm 0.00000004$ , with the uncertainty being  $\pm 1$  phase bins. With this TOA and the ATNF ephemeris, we infer a phase difference of  $\text{TOA}_{\text{radio}} - \text{TOA}_{\text{X}} = 0.07 \pm 0.11$  cycles, where the uncertainty is dominated by uncertainties in the ephemeris (see Figure 2).

### 2.2. Spectral Analysis

Spectral fitting was done in `sherpa` (Refsdal et al. 2009). For the fits, we only included events between 0.32–1.1 keV, as the response below 320 eV is not well understood. This leaves 1003 source and 267 background counts. We follow recommendations in modeling the low-energy background with a power-law instead of subtracting it (although given that the expected background in the source area is less than 1 count, it does not influence the results). We binned the source counts such that each bin contained at least 25 counts and was at least 29 eV wide, so that  $\chi^2$  statistics are a good approximation, and we do not oversample the instrumental resolution of  $\sim 100$  eV.

We tried three main source models: a thermal blackbody, a non-thermal power law, and a simple neutron-star atmosphere model (NSA; Pavlov, Shibano, & Zavlin 1991; Zavlin, Pavlov, & Shibano 1996), all modified by interstellar absorption (using `xsphabs`; the parameters changed only minutely with other choices, such as `xstbabs` and `xswabs`). We tried NSA models with and without a strong magnetic field; for both, we fixed the mass and radius of the neutron star at  $1.4 M_\odot$  and 10 km, respectively. Our results are summarized in Table 1 (there and below, temperatures and radii refer to those measured by a distant observer).

The NSA models gave reasonable fits, but implied implausibly small distances:  $33_{-18}^{+22}$  and  $160_{-60}^{+110}$  pc for the  $B = 0$  and  $B = 10^{13}$  G models, respectively. A power-law model gave a significantly worse fit than the thermal models ( $\chi^2 = 76.9$  vs. 45.1 for 67 dof). We found that, similar to the INs, a simple blackbody gave a good fit (Fig. 3) and the most reasonable parameters.<sup>5</sup> In what follows, we use that as our baseline model. We find there is significant covariance between the fitted parameters, which, within  $1\sigma$ , leads to changes in absorption of  $4 \times 10^{20} \text{ cm}^{-2}$  and in temperature of  $\sim 5$  eV. To explore the influence of the absorption column, we also tried fits where we held  $N_{\text{H}}$  fixed at 1 or 10 times the dispersion measure ( $70 \text{ cm}^{-3} \text{ pc} = 2.1 \times 10^{20} \text{ cm}^{-2}$ ). These fits were somewhat worse than those with  $N_{\text{H}}$  free, but still had reduced  $\chi^2$  less than 1.

To constrain any additional non-thermal emission, we tried adding a power law to the blackbody. We found it had negligible effect on the parameters, and, assuming  $\Gamma = 3$ , we infer a  $1\sigma$  upper limit of the photon rate of

<sup>5</sup> With the blackbody model and the observed 0.32–1.1 keV count rate of  $0.056 \text{ s}^{-1}$ , the expected count rate for ROSAT PSPC is  $0.027 \text{ s}^{-1}$  (estimated using the Portable, Interactive Multi-Mission Simulator [PIMMS]; <http://heasarc.gsfc.nasa.gov/Tools/w3pimms.html>). Thus, most likely PSR J0726 is responsible for all of the flux of 1RXS J072559.8–261229.

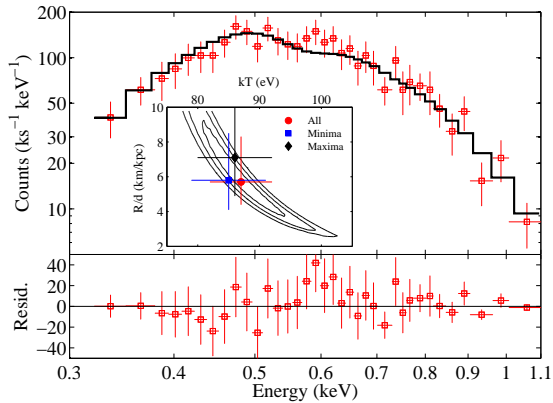


FIG. 3.— The best-fit blackbody model along with residuals (lower panel). Inset: best-fit contours of  $kT$  vs. normalization  $R/d$ , with 1-, 2-, and 3- $\sigma$  joint confidence contours ( $\Delta\chi^2 = 2.30, 6.17, 11.8$ ). The best-fit value is the red circle, while the blue square and black diamond are for the combined minima and maxima, respectively.

$7 \times 10^{-6} \text{ s}^{-1} \text{ cm}^{-2} \text{ keV}^{-1}$  at 1 keV, corresponding to  $\lesssim 3\%$  of the flux in the 0.32–1.1 keV band.

We also tried fitting the spectrum of PSR J0726 with a model that included an additive Gaussian line, in order to constrain the presence of absorption features similar to those seen for the INSs, which have equivalent widths of up to several 100 eV (Haberl 2007; van Kerkwijk & Kaplan 2007). We fixed the full width at half maximum (FWHM) of the line to 0.1 keV, comparable to the energy resolution of the back-illuminated ACIS-S3 CCD, and varied the line energy between 0.3 keV and 1.1 keV, fitting only for its amplitude (allowing both positive and negative amplitudes). As expected from Fig. 3, we did not find evidence for any absorption line. The largest improvement in the fit occurs near 0.6 keV, for an emission line with a height of 35%, but even this reduces  $\chi^2$  by only 4, which is not significant given our number of trials (based on simulations, we estimate a false-alarm probability of  $\sim 30\%$ ). We infer a 68%-confidence upper limit of 50 eV to the equivalent width of any feature.

Finally, we looked for phase-resolved trends in two ways. First, we determined the median energy as a function of pulse phase (upper panel in Figure 2), finding little change except perhaps a hint of hardening at the maximum that is coincident with the radio peak, although given the current statistics this is not significant (the  $\chi^2$  for the median energy is 9 for 15 degrees-of-freedom). Second, we separated the data into two bins: one containing the two maxima and one the two minima, each with 50% of the exposure time. From our fit (Table 1 and Figure 3), we find negligible difference in temperature between the maxima and minima, consistent with the lack of change seen in median energy. Thus, the pulsations appear to reflect mostly changes in emitting area.

### 2.3. Spatial Analysis

To check for possible extended emission, e.g., from a pulsar wind nebula, we compared our observations with a simulated point-spread function (PSF), created using *ChART* (the *Chandra* Ray Tracer) and *MARX* (version 4.5.0), for a spectrum consistent with our best-fit blackbody. We find good agreement for radii  $\geq 2$  pixels ( $1''$ ), although with only  $\approx 180$  counts at these radii, the con-

straints are not strong. Oddly, the two bins at the smallest radii, 0–0.5 pixels and 0.5–1.0 pixels, had some deviations, with the model PSF underpredicting the counts in the first bin by about  $6\sigma$  (30%), and overpredicting the second by about  $4\sigma$  (26%). Since it is unlikely that the pulsar is more centrally concentrated than a point-source, we probably are simply reaching the limits in the model (we experimented with the *Chandra* processing, turning off pixel position randomization, but found that this made little difference). We conclude that there is no evidence for extended emission on scales of  $\gtrsim 1''$ .

## 3. DISCUSSION

Regardless of the path by which PSR J0726 and the INSs got to their present states, we can examine how closely their current properties resemble each other and whether the unique information from either helps understand the thermal emission from this class of neutron stars as a whole. Furthermore, we can see how PSR J0726 might help us understand the evolution of high- $B$  pulsars and the origin of the INSs. We consider these in turn.

### 3.1. Comparison with the INSs

PSR J0726 was selected to be similar to the INSs in having a long spin-period,  $P > 3$  s, and strong magnetic field,  $B = (1 - 3) \times 10^{13}$  G. With a thermal spectrum with  $kT = 87 \pm 5$  eV, and  $R \approx 6$  km (at the nominal distance of  $\sim 1$  kpc in the Gould Belt), its X-ray properties are similar as well (indeed, it would be classified as an INS based on these). Its spectrum has no evidence for absorption, unlike RX J1308.6+2127, which has strong absorption (Haberl et al. 2003) while having a very similar magnetic field and a slightly higher temperature ( $B = 3.4 \times 10^{13}$  G, Kaplan & van Kerkwijk 2005b;  $kT = 102$  eV, Schwöpe et al. 2007). However, RX J0720.4–3125, another INS with a similar if slightly lower field ( $B = 2.4 \times 10^{13}$  G, Kaplan & van Kerkwijk 2005a), had weak absorption, with an equivalent width of  $\sim 5$  eV, which we would not be able to detect, when its temperature was most similar to PSR J0726 ( $kT = 86$  eV, Haberl et al. 2004). Intriguingly, this source changed, developing much stronger absorption while becoming hotter ( $kT = 94$  eV, de Vries et al. 2004; Haberl et al. 2006; van Kerkwijk et al. 2007). Taking our inferred temperature at face value, it is thus possible that PSR J0726 emits identically to an INS of the same temperature and dipole magnetic field strength. If so, at higher sensitivity it may show weak absorption at  $\sim 300$  eV. (We caution, however, that the dependencies of absorption energy and strength on temperature and magnetic field strength remain puzzling for the INSs as a class; Kaplan & van Kerkwijk 2009a,b.)

The inferred luminosity  $L_X = 1.5 \times 10^{32} d_{\text{kpc}}^2 \text{ erg s}^{-1}$  (0.32–1.1 keV) is about half the rotational energy loss rate  $\dot{E} = 4\pi^2 I \dot{P} / P^3 = 2.8 \times 10^{32} \text{ erg s}^{-1}$  (for a moment of inertia  $I = 10^{45} \text{ g cm}^2$ ). This is on the low side of what is seen for the INSs ( $L_X \sim (0.5 \dots 100) \dot{E}$ ), possibly just a consequence of PSR J0726 having a shorter period for the same  $B$  (for dipole spin-down,  $\dot{E} \propto B^2 / P^4$ ). It is much larger than the non-thermal emission typically observed for rotation-powered pulsars ( $L_X \approx 10^{-3} \dot{E}$ , Becker & Trümper 1997), although we cannot exclude



TABLE 1  
RESULTS OF X-RAY FITS TO PSR J0726–2612

Model	$N_{\text{H}}$ ( $10^{20} \text{ cm}^{-2}$ )	$\Gamma$ or $kT$ (N/A or eV)	$A$ or $R/d^a$ ( $10^{-5} \text{ s}^{-1} \text{ cm}^{-2} \text{ keV}^{-1}$ or $\text{km kpc}^{-1}$ )	$F_{\text{abs}}^b \times 10^{-13}$ ( $\text{erg s}^{-1} \text{ cm}^{-2}$ )	$F_{\text{unabs}}^b \times 10^{-13}$ ( $\text{erg s}^{-1} \text{ cm}^{-2}$ )	$\chi^2/\text{DOF}$
Blackbody .....	$8^{+4}_{-3}$	$87 \pm 5$	$5.7^{+2.6}_{-1.3}$	4.5	12.9	45.1/67
Blackbody .....	2	$95 \pm 2$	$3.5^{+0.3}_{-0.2}$	4.5	5.6	48.1/68
Blackbody .....	21	$74 \pm 2$	$17.1^{+1.5}_{-1.4}$	3.6	33.8	55.0/68
NSA ( $B = 0$ ) .....	$14^{+9}_{-4}$	$22 \pm 3$	$307^{+370}_{-122}$	4.2	22.7	52.8/67
NSA ( $B = 10^{13} \text{ G}$ )	$12^{+4}_{-4}$	$42 \pm 4$	$63^{+39}_{-24}$	4.3	19.2	52.8/67
Power Law ( $\Gamma$ free)	$20^{+4}_{-4}$	$6.4 \pm 0.4$	$7.6^{+1.0}_{-0.8}$	4.2	60.6	76.9/67
Power Law ( $\Gamma = 3$ )	$0^{+0.1}_{-0.1}$	3	$9.0^{+0.7}_{-0.2}$	3.2	3.2	195/66
Blackbody phase-resolved:						
Minima <sup>c</sup> .....	$9^{+5}_{-4}$	$85 \pm 6$	$5.8^{+2.7}_{-1.7}$	3.3	8.5	24.3/37
Maxima <sup>c</sup> .....	$9^{+5}_{-4}$	$86 \pm 6$	$7.1^{+3.5}_{-2.2}$	5.1	13.2	47.1/51

NOTE. — Quantities without uncertainties were held fixed during the fit. All uncertainties are for 1- $\sigma$  confidence, and all other parameters were allowed to vary during the calculation of the uncertainties.

<sup>a</sup> For the NSA models, the mass is fixed to  $1.4 M_{\odot}$  and the radius is fixed at 10 km, so the uncertainties calculated for  $R/d$  are based on the best-fit distance. The normalization of the power-law model  $A$  is the photon rate at an energy of 1 keV.

<sup>b</sup> The fluxes are given in the 0.32–1.1 keV band and are given both as observed and corrected for absorption.

<sup>c</sup> Phase-resolved spectroscopy using a blackbody model. The two phase bins each include 50% of the data, and were fit simultaneously with the same absorption.

that PSR J0726 has a similar non-thermal component: our  $1\sigma$  upper limit of 3% of the 0.32–1.1 keV flux for the contribution of a power-law with  $\Gamma = 3$  (a value typical for pulsars) implies  $L_{\text{PL}} \lesssim 0.015 d_{\text{kpc}}^2 \dot{E}$ .

The pulse properties of PSR J0726 also echo those of the INs, which show smooth profiles dominated by the fundamental or the first harmonic. The pulse fraction of  $27 \pm 5\%$  is a little larger than the  $\sim 1$  to 18% seen for the INs (Haberl 2007), but it is not dramatically different. We note that without the radio period, we might have actually identified the pulse period of PSR J0726 as half of the true value. The lack of temperature variation is somewhat strange (cf. up to 10% changes in  $kT$  over the pulse of RX J1308.6+2127, for example; Schwöpe et al. 2005), as, naively, it implies that we are seeing changes in projected area of large regions of similar temperature with anything in between so much colder that it does not contribute. It may be that instead the whole surface emits at more or less a uniform temperature, and that the pulsations reflect anisotropies in the emission, perhaps associated with the strong magnetic field. The same may hold for the INs, which typically also show only modest changes in temperature with pulse phase.

A possible difference with the INs is that PSR J0726 has an order-of-magnitude smaller characteristic age. This may again be a consequence of its shorter period for the same  $B$  (for dipole spin-down,  $\tau \propto (P/B)^2$ ), but might also point to an evolutionary difference (see below). Another characteristic of INs is that they have faint optical counterparts, but with optical/UV fluxes a factor of 6–50 above the extrapolation of the X-rays. This is in contrast to middle-aged pulsars such as PSR B0656+14 and Geminga, which have ultraviolet fluxes that are more consistent with the X-ray extrapolations (Shibanov et al. 2005; Kargaltsev et al. 2005). It will be interesting to see whether PSR J0726 has an excess or not.

Of course, the most glaring difference between PSR J0726 and the INs is the radio emission. Numerous

searches have yet to find confirmed radio emission (coherent or bursty) from the INs (Kondratiev et al. 2009, and references therein). This may be a result of their location near the pulsar “death line,” or more simply a consequence of their narrow radio beams: the 50% width of the radio pulse from PSR J0726 is  $< 1\%$  of the pulse period (consistent with general trends for long-period pulsars) so the chance of missing the radio pulse is large.

Overall, we conclude that with the exceptions of its radio emission and characteristic age, the properties of PSR J0726 agree with those of the INs. Based on the compilations of Kaplan & van Kerkwijk (2009b), Zhu et al. (2011), and references therein, it is the best pulsar analog to the INs to date.

### 3.2. Implications for the Evolution of High- $B$ Neutron Stars

In order to look for evolutionary trends, we can compare PSR J0726 to sources with similar properties in the  $P$ - $\dot{P}$  diagram, as well as with the evolution expected from the work of Pons et al. (2009), which seems to explain the origins of the INs (Fig. 1). A first comparison is with INs of similar field and temperature, RX J0720.4–3125 and RX J1308.6+2127. As mentioned, the main difference is that the characteristic age of PSR J0726 is 200 kyr, while those of the INs are  $> 2$  Myr. This could imply that the true age of PSR J0726 is closer to its characteristic age than is the case for the INs, and maybe that it has undergone less  $B$  decay. This is consistent with the models of Pons et al. (2009):  $3 \times 10^{13} \text{ G}$  is near the dividing line where field-decay becomes important, and the true age is expected to be no more than a factor 2 shorter than the characteristic age (see Fig. 1). Taking the models at face value, one infers that PSR J0726 was born with a dipole field of just below  $10^{14} \text{ G}$ , while most INs would have had a field about a factor 2 stronger.

As a second comparison, we can compare PSR J0726 with two X-ray-detected objects that have almost the

same period: the modest- $B$  INS RX J0420.0–5022 ( $1.0 \times 10^{13}$  G, Kaplan & van Kerkwijk 2011), and the high- $B$  pulsar PSR J1718–3817 ( $7.4 \times 10^{13}$  G, Zhu et al. 2011). The former is very similar to PSR J0726, with the main difference being that it is cooler ( $kT \approx 45$  eV). From the evolutionary tracks, it seems most likely RX J0420.0–5022 initially simply had even lower magnetic field strength, which decayed by a factor  $\sim 2$  or so, and that, like PSR J0726, its true age is at most a factor 2 shorter than its characteristic age of 2 Myr.

From the evolutionary tracks, PSR J1718–3817 would be a good candidate progenitor for INSs like RX J0720.4–3125, and indeed it has a largely thermal spectrum consistent with a blackbody with a significantly hotter temperature ( $kT \approx 190$  eV), suggestive of ongoing field decay. However, the emitting radius of  $\sim 2$  km and pulsed fraction of  $\sim 50\%$  differ from those found for the INSs (and PSR J0726), and are more reminiscent of even younger high- $B$  pulsars like PSR J1119–6127 (Gonzalez et al. 2005), which also have high pulsed fractions and smaller radii (although distance and fitting uncertainties make the radii for all these objects poorly constrained). It may be that this reflects some combination of ongoing  $B$  decay and non-thermal heating; all these younger, strong-field objects have substantially larger spin-down energy losses. Alternatively, the stronger field may lead to more anisotropic emission.

Overall, it seems that the INSs and high- $B$  pulsars form a single family (also see Kaspi 2010 for further discussion), with initial fields that were stronger than their current ones, and that caused rapid initial spin-down. The long periods for the slower spinning objects also imply low rotational energy losses and thus weak non-thermal emission. Combined with some additional heating due to field decay, this makes the thermal emission stand out more than it would in normal pulsars.

A continuing puzzle, however, is the difference with the magnetars (Ng & Kaspi 2011), which occupy similar parts of the  $P$ - $\dot{P}$  diagram, but are clearly much more strongly affected by magnetic field decay. It may be that those were born with much stronger toroidal components to the field (which affect the spin-down only indirectly, via the more rapid field decay). In any case, there may be a smooth continuum, given objects like PSR J1846–0258 ( $B = 4.9 \times 10^{13}$  G) which exhibited a sudden, magnetar-like X-ray outburst (Gavriil et al. 2008; Kumar & Safi-Harb 2008; Ng et al. 2008), the INS RX J0720.4–3125 that exhibited a possible magnetic

reconfiguration (de Vries et al. 2004; van Kerkwijk et al. 2007), the transient magnetar XTE J1810–197 that was detected in outburst (Ibrahim et al. 2004) but in quiescence appears more like an INS (Bernardini et al. 2011), or the putative low- $B$  magnetar SGR 0418+5729 ( $< 8 \times 10^{12}$  G; Rea et al. 2010; Turolla et al. 2011).

#### 4. OUTLOOK

Our *Chandra* observations show that the relatively nearby high- $B$  pulsar PSR J0726–2612 has properties similar to those of the INSs, showing analogous thermal emission and similar smooth pulsations. Because of its radio emission, PSR J0726–2612 may help us clarify the nature of the emission and the pulsations. First, for many radio pulsars the observed polarization position angle curve is well described by the rotating vector model (Radhakrishnan & Cooke 1969), in which the position angle is assumed to be aligned with a dipolar magnetic field. Using this model, one can infer the (mis)alignment between the spin and magnetic axes, as well as the angle between the spin axis and line-of-sight. Using such a model for PSR J0726 and combining it with fits to the X-ray light-curve will help resolve the ambiguities that limited lightcurve analyses for INSs (Braje & Romani 2002; Zane & Turolla 2006; Ho 2007). Second, unlike for the INSs where only X-ray and optical astrometry (both of limited precision) are possible, for PSR J0726 traditional radio techniques are available (proper motions with the Very Large Array, and potentially parallaxes with the Very Long Baseline Array). This means that even though the likely distance is  $\sim 1$  kpc, which would be well outside of reach for an optical parallax, we can hope for a geometric distance measurement for PSR J0726 that would constrain its emitting radius.

We thank the referee for helpful comments. Support for this work was provided by the US National Aeronautics and Space Administration (NASA) through *Chandra* award GO1-12080X and grant NNX08AX39G, and by the Canadian Natural Sciences and Engineering Research Council (NSERC). This paper includes archived data obtained through the Australia Telescope Online Archive and the CSIRO Data Access Portal (<http://datanet.csiro.au/dap/>). We thank W. van Straten for assistance in interpreting those data. We made extensive use of SIMBAD and ADS.

*Facilities:* CXO (ACIS)

#### REFERENCES

- Becker, W. & Trümper, J. 1997, *A&A*, 326, 682  
 Bernardini, F., Perna, R., Gotthelf, E., Israel, G. L., Rea, N., & Stella, L. 2011, *ArXiv e-prints*  
 Braje, T. M. & Romani, R. W. 2002, *ApJ*, 580, 1043  
 Buccheri, R., et al. 1983, *A&A*, 128, 245  
 Burgay et al. 2006, *MNRAS*, 368, 283  
 Cordes & Lazio. 2002, *astro-ph/0207156*  
 de Vries, C. P., Vink, J., Méndez, M., & Verbunt, F. 2004, *A&A*, 415, L31  
 Faucher-Giguère, C.-A. & Kaspi, V. M. 2006, *ApJ*, 643, 332  
 Garmire, G. P., Bautz, M. W., Ford, P. G., Nousek, J. A., & Ricker, G. R. 2003, *Proc. SPIE*, 4851, 28  
 Gavriil, F. P., Gonzalez, M. E., Gotthelf, E. V., Kaspi, V. M., Livingstone, M. A., & Woods, P. M. 2008, *Science*, 319, 1802  
 Gonzalez, M. E., Kaspi, V. M., Camilo, F., Gaensler, B. M., & Pivovarov, M. J. 2005, *ApJ*, 630, 489  
 Gonzalez, M. E., Kaspi, V. M., Lyne, A. G., & Pivovarov, M. J. 2004, *ApJ*, 610, L37  
 Haberl, F. 2007, *Ap&SS*, 308, 181  
 Haberl, F., Schwope, A. D., Hambaryan, V., Hasinger, G., & Motch, C. 2003, *A&A*, 403, L19  
 Haberl, F., Turolla, R., de Vries, C. P., Zane, S., Vink, J., Méndez, M., & Verbunt, F. 2006, *A&A*, 451, L17  
 Haberl, F., Zavlin, V. E., Trümper, J., & Burwitz, V. 2004, *A&A*, 419, 1077  
 Ho, W. C. G. 2007, *MNRAS*, 380, 71  
 Ibrahim, A. I., et al. 2004, *ApJ*, 609, L21  
 Kaplan, D. L. 2008, *AIPC*, 983, 331, *arXiv:0801.1143*  
 Kaplan, D. L. & van Kerkwijk, M. H. 2005a, *ApJ*, 628, L45  
 —. 2005b, *ApJ*, 635, L65  
 —. 2009a, *ApJ*, 692, L62  
 —. 2009b, *ApJ*, 705, 798

- . 2011, *ApJ*, 740, L30
- Kaplan, D. L., van Kerkwijk, M. H., & Anderson, J. 2007, *ApJ*, 660, 1428
- Kargaltsev, O. Y., Pavlov, G. G., Zavlin, V. E., & Romani, R. W. 2005, *ApJ*, 625, 307
- Kaspi & McLaughlin. 2005, *ApJ*, 618, L41
- Kaspi, V. M. 2010, *Proceedings of the National Academy of Science*, 107, 7147
- Kondratiev, V. I., McLaughlin, M. A., Lorimer, D. R., Burgay, M., Possenti, A., Turolla, R., Popov, S. B., & Zane, S. 2009, *ApJ*, 702, 692
- Kumar, H. S. & Safi-Harb, S. 2008, *ApJ*, 678, L43
- Manchester, R. N., Hobbs, G. B., Teoh, A., & Hobbs, M. 2005, *AJ*, 129, 1993
- McLaughlin, M. A., et al. 2007, *ApJ*, 670, 1307
- Motch, C., Pires, A. M., Haberl, F., Schwope, A., & Zavlin, V. E. 2009, *A&A*, 497, 423
- Motch, C., Sekiguchi, K., Haberl, F., Zavlin, V. E., Schwope, A., & Pakull, M. W. 2005, *A&A*, 429, 257
- Ng, C.-Y. & Kaspi, V. M. 2011, in *American Institute of Physics Conference Series*, Vol. 1379, American Institute of Physics Conference Series, ed. E. Göğüş, T. Belloni, Uuml. Ertan, 60–69
- Ng, C.-Y., Slane, P. O., Gaensler, B. M., & Hughes, J. P. 2008, *ApJ*, 686, 508
- Pavlov, G. G., Shibano, I. A., & Zavlin, V. E. 1991, *MNRAS*, 253, 193
- Pons, J. A., Miralles, J. A., & Geppert, U. 2009, *A&A*, 496, 207
- Popov, S. B., Pons, J. A., Miralles, J. A., Boldin, P. A., & Posselt, B. 2010, *MNRAS*, 401, 2675
- Popov, S. B., Turolla, R., Prokhorov, M. E., Colpi, M., & Treves, A. 2005, *Ap&SS*, 299, 117
- Radhakrishnan, V. & Cooke, D. J. 1969, *Astrophys. Lett.*, 3, 225
- Ransom, S. M. 2001, PhD thesis, Harvard University
- Rea, N., et al. 2010, *Science*, 330, 944
- Refsdal, B., et al. 2009, in *Proceedings of the 8th Python in Science conference (SciPy 2009)*, ed. G. Varoquaux, S. van der Walt, & J. Millman, 51–57
- Schwope, A. D., Hambaryan, V., Haberl, F., & Motch, C. 2005, *A&A*, 441, 597
- . 2007, *Ap&SS*, 308, 619
- Shibanov, Y. A., Sollerman, J., Lundqvist, P., Gull, T., & Lindler, D. 2005, *A&A*, 440, 693
- Tetzlaff, N., Eisenbeiss, T., Neuhaeuser, R., & Hohle, M. M. 2011, *MNRAS*, in press, arXiv:1107.1673
- Tetzlaff, N., Neuhaeuser, R., Hohle, M. M., & Maciejewski, G. 2010, *MNRAS*, 402, 2369
- Turolla, R., Zane, S., Pons, J. A., Esposito, P., & Rea, N. 2011, *ApJ*, in press, arXiv:1107.5488
- van Kerkwijk, M. H. & Kaplan, D. L. 2007, *Ap&SS*, 308, 191
- . 2008, *ApJ*, 673, L163
- van Kerkwijk, M. H., Kaplan, D. L., Pavlov, G. G., & Mori, K. 2007, *ApJ*, 659, L149
- Voges, W. et al. 1999, *A&A*, 349, 389
- Walter, F. M. 2001, *ApJ*, 549, 433
- Weisskopf, M. C., Tananbaum, H. D., Van Speybroeck, L. P., & O'Dell, S. L. 2000, *Proc. SPIE*, 4012, 2
- Zane, S. & Turolla, R. 2006, *MNRAS*, 366, 727
- Zavlin, V. E., Pavlov, G. G., & Shibano, Y. A. 1996, *A&A*, 315, 141
- Zhu, W., Kaspi, V. M., Dib, R., Woods, P. M., Gavril, F. P., & Archibald, A. M. 2008, *ApJ*, 686, 520
- Zhu, W. W., Kaspi, V. M., McLaughlin, M. A., Pavlov, G. G., Ng, C.-Y., Manchester, R. N., Gaensler, B. M., & Woods, P. M. 2011, *ApJ*, 734, 44